

## METHODS

## Machine learning classification of normal vs. age-related macular degeneration OCT images

R. Loganathan<sup>1</sup>, S. Latha<sup>1\*</sup> and Kirubanandan Shanmugam<sup>2,3</sup>

<sup>1</sup>Department of Electronics and Communication Engineering, SRM Institute of Science and Technology, Chennai, India

<sup>2</sup>Department of Biotechnology, Sree Sastha Institute of Engineering and Technology, Chennai, India

<sup>3</sup>International Conference on Modern Advancement in Diagnosis and Treatment of Clinical Cancer, Sree Sastha Institute of Engineering and Technology, Chennai, India

**\*Correspondence:**

S. Latha,  
lathas3@srmist.edu.in

**Received:** 08 May 2021; **Accepted:** 03 June 2021; **Published:** 19 June 2021

The macula is a small area of the retina which is especially very important for good eyesight. The age-related macular degeneration (AMD) is a type of visual impairment that can cause blindness or even loss of eyesight. AMD was a dangerous and progressing chronic disease that affects people over the age of 60 years. One of the most common symptoms of this condition is the appearance of a type of extracellular material called the drusen. Detecting this condition using an imaging technique known as optical coherence tomography (OCT) can help to prevent further damage to the eyes. The motivation behind this work is to test machine learning (ML) with OCT images for the identification of retinal disease. OCT retinal images consist of normal retina and AMD. ML algorithms were used to classify 261 OCT images to determine if the person was normal or macular. The proposed method for diagnosing between diseased and healthy conditions has a classification accuracy that considerably exceeds beyond the current state of the art. This work will be used in developing further ML concepts in the diagnosis of ocular disorders and diseases.

**Keywords:** optical coherence tomography, age-related macular degeneration, machine learning

### Introduction

By there will be 2.1 billion people over the age of 60 years in this world. The population with more than 80 years of age is likely to be 3-fold between 2020 and 2050, which is estimated to be 426 million (1). An eye condition known as age-related macular degeneration (AMD) can degrade over time. It is a major effect of serious and stable eyesight failure in people aged more than 60 years (2). Light signals are converted into neurological signals from the inward layer of the eyes called the retina. It is made up of several rod and cone pigments, and that is bound to dim light as well as color vision. The retina has a few layers of disinfectant and physiologic concern. In general, damage to particular layers leads to various deformities, along with vision loss. Optical coherence tomography (OCT) continues to be an

important device used for diagnosing various retinal diseases such as blindness, AMD, macular edema, macular hole (MH), chronic glaucoma, retinal cysts, diabetic retinopathy (DR), and central serous retinopathy (CSR).

The visual system includes a distinct opportunity to examine the ageing process and the problems in evolving treatments for age-related eye diseases. This article proposes several different approaches in ML algorithms to resolve such problems. To act as the focus of the investigation and to evaluate the suggested ideas, retinal imaging screening was used as an exemplary application domain, more specifically, the detection of AMD by classifying images as AMD normal or abnormal disease.

Koh Jew et al. used a random forest (RF) classifier for the classification of normal from abnormal (DR, AMD, and glaucoma) images by using 404 normal and 1,082 abnormal

fundus retinal images. The 2D continuous wavelet transform was used to extract energy and entropy features without segmenting and achieved high accuracy, able to categorize three different classes of fundus images. According to the authors, their technique has a classification accuracy of 92.48%. The fundus images of glaucoma are centered on the optic disc, while the fundus images of AMD, DR, and normal are centered on the macula that can also affect the performance of the classifier (3).

Wang, Yu et al. proposed a multiclass model using linear configuration patterns (LCPs) and sequential minimum optimization (SMO) classification algorithm to distinguish between AMD, healthy macula, and diabetic macular edema (DME), achieving an overall accuracy of 98.0% for all three samples of OCT images (4).

Garcia et al. proposed a new ML model mixed up with image processing and mathematical morphology to create the support vector machine (SVM). Drusen form is detected in the retina region by the image segmentation process. The invariant moment features are obtained from fundus images as vectors, which are used by SVM to classify the fundus images as positive or negative for drusen. It identified the existence of drusen within retina as well as diagnosed AMD automatically. The performances obtained are satisfactory, but the accuracy threshold of 95% cannot be exceeded.

Support vector machine, k-nearest neighborhood, and ML algorithms were evaluated to classify images with and without fat deposits, which yielded better accuracy and sensitivity (5). A comparison of the three methods of feature extraction was performed and, in addition to distinguishing features, HMM and SVM classifiers were used to identify whether signal is Parkinson's or not (6). The compressed sensing (CS) method is used for compressing therapeutic images. Random permutation coefficient based CS is used to compress medical images. This method maintains a decent sparsely of the restored image for a high-quality flattened image (7). Texture analysis on segmented images is performed using the AM-FM technology. The current values of the amplitude and frequency of each image sample are obtained and quantized. It is then compared to a standard tissue sample to determine if the artery is normal or abnormal (8). In our study, AMD was detected based on fundus retinal images in the FRI database using an ML system implemented in MATLAB. The SVM classification accuracy is greater (>93%) than other ML classifiers (9).

## Methodology

The OCT image database (OCTID) consists of AMD and normal images, which will help to classify it more efficiently and accurately. From normal retina and AMD, OCT images can vary in level for equal disease; a professional or an expert in ML is required to assist the clinician to classify images.

## Dataset

This database contains over 500 spectral OCT volumetric scans categorized into five subsets: 206 images of normal retina, 55 images of AMD, 102 images of macular rupture, 107 images of diabetic retinopathy, and 102 images of central serous retinopathy. This dataset consists of different retinal OCT images that can be found in the OCTID by Peyman Gholami et al. (10), an open-source dataset. In these images, a raster scan protocol was used, with a 2 mm scan length, containing  $512 \times 1,024$  pixels, collected using a Cirrus HD-OCT machine at Sankara Nethralaya (SN) eye hospital in Chennai, India. The scanned images were resized to  $500 \times 750$  pixels. The normal subset and AMD subset of the database were considered two classes, namely, normal retinal and AMD retinal, which are used in this experiment for the binary classification of OCT images using ML. **Figure 1** represents the images of the two classes of OCT images.

## Histogram

The basic step of this method requires the image plotter to convert the signal into a digital image or images can be captured in RGB color format from online medical data of fundus images of the library or clinical OCT images, and then converted into grayscale. **Figure 1A** shows a normal retinal image, and **Figures 1B, C** show wet and dry AMD retinal images, respectively. Histograms of the normal retinal image and AMD retinal image are shown in **Figures 2A, B**, respectively.

The research methods include the steps such as data collection of AMD and normal OCT images, processing, selection of a pre-trained ML model, and testing dataset, and test data of normal or AMD OCT images are classified by ML-based algorithms. For AMD and normal OCT images, the efficacy of various ML algorithms is compared. The specific steps are given in **Figure 3**.

## Data collection and processing

The training and testing sets were obtained from the OCTID, which consists of AMD and normal subsets alone. From the splitting python code, we obtained 209 images to train the classifier model and 52 images for testing. The system assigns

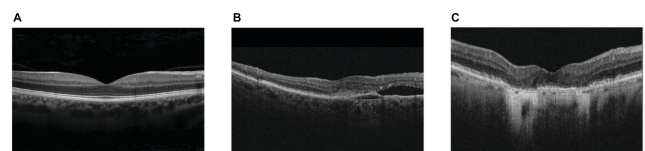


**FIGURE 1 | (A)** A normal retinal, **(B)** wet AMD retinal, and **(C)** dry AMD retinal.

a value of 0 to normal images and 1 to AMD images for the study of binary classifications. Classifier performance can be improved by employing several kernels. Each OCT image was processed as a  $320 \times 320 \times 3$  image, where 3 is the number of color channels, to ensure compatibility with ML-based architecture. The processed normal and AMD images are shown in **Figures 4A, B**, respectively.

### Training and classification

The selected normalized function can be divided into two types, namely, 80% of data are used for training the model and the remaining 20% of data are used for validating the accuracy of a pre-trained model. Once the formation separation is complete, the proposed data from the test data are training data for binary classification algorithms. There are several algorithms suitable to be used as binary classification algorithms including K-nearest neighbour (KNN), SVM, RF, decision tree (DT), logistic regression (LR), and naive Bayes (NB). Test dataset is applied to these different ML models, the accuracy of each classifier

model is obtained, and the best model is predicted from the results obtained.

### Discussion

Training set and series of tests were incorporated in the testing dataset comprising OCT images from AMD and normal retina. The image was processed to  $320 \times 220 \times 3$  pixels, where 3 denotes the number of color channels and ensures interoperability with ML-type algorithms. The dataset, training, and testing sets for the OCTID are shown in **Table 1**. Experimental dataset of OCT images from AMD and normal retina included a training set and series of tests. To maintain compatibility with the ML-based algorithms, all OCT image was processed as a  $320 \times 220 \times 3$  image, where the number of color channels is 3. **Table 1** shows the dataset, training, and test sets for AMD and normal OCT images.

The dataset, training, and testing set of AMD and normal retinal images are shown in **Figures 5A-C**. In this work, value 0 is assigned to normal retinal images and value 1 is assigned to AMD retinal images.

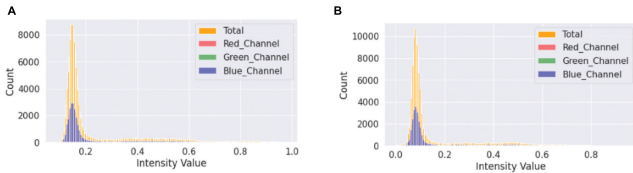


**FIGURE 2 | (A)** A normal retinal, **(B)** wet AMD retinal, and **(C)** dry AMD retinal.

**TABLE 1 |** OCTID of AMD and normal retina dataset, training, and testing set.

Category	Dataset	Training Set	Testing Set
Normal retina	206	165	41
AMD	55	43	12
Total image	261	208	53

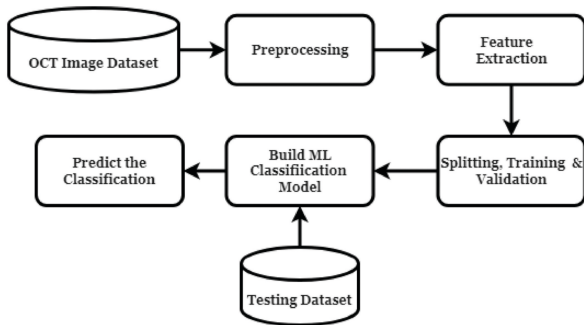


**FIGURE 3 |** Overall view of the proposed method.

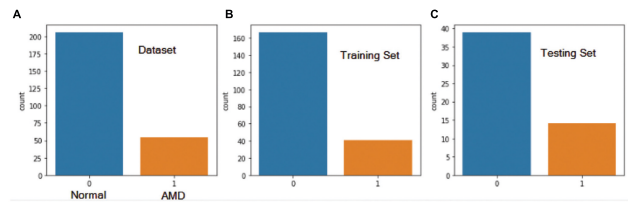


**FIGURE 5 | (A)** Datasets, **(B)** training set data, and **(C)** testing set data.

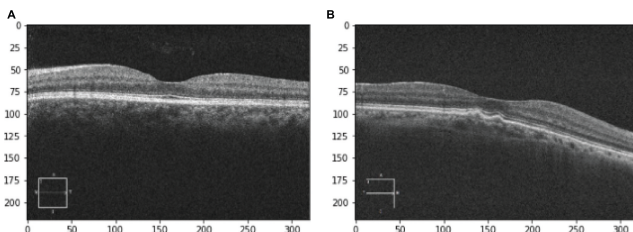


**FIGURE 4 | (A)** A normal OCT image and **(B)** AMD OCT image with  $320 \times 220$  pixels.

**TABLE 2 |** ML models' classification metrics.

	Accuracy	Precision	Recall	F1	ROC_AUC
Logistic regression	0.962264	0.833333	1.000000	0.909091	0.976744
Support vector machines	0.943396	0.916667	0.846154	0.880000	0.910577
Decision trees	0.962264	0.833333	1.000000	0.909091	0.976744
Random forest	0.981132	0.916667	1.000000	0.956522	0.988095
Naive bayes	0.943396	0.833333	0.909091	0.869565	0.930736
K-Nearest neighbor	0.886792	0.500000	1.000000	0.666667	0.936170

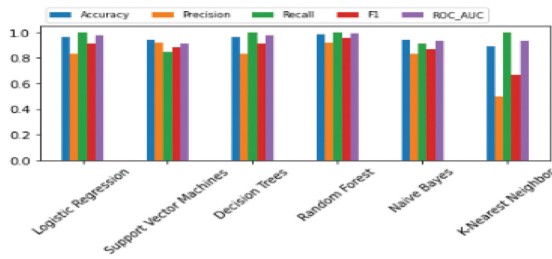


**FIGURE 6** | Comparison of metrics classification report for different ML models.

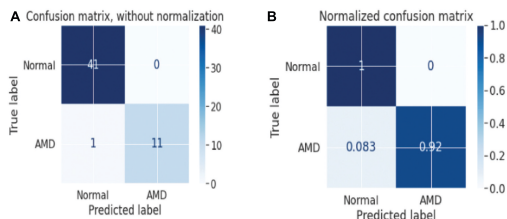
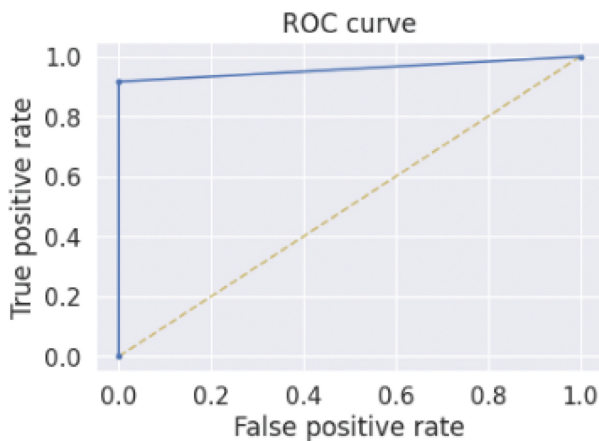


**FIGURE 7** | (A) Confusion matrix for RF model without normalization and (B) confusion matrix for RF model with normalization.

	precision	recall	f1-score	support
0	0.98	1.00	0.99	41
1	1.00	0.92	0.96	12
accuracy			0.98	53
macro avg	0.99	0.96	0.97	53
weighted avg	0.98	0.98	0.98	53

**FIGURE 8** | Classification report of RFML model for normal (0) and AMD (1) images.



Area under curve, AUC = 0.9583333333333333

**FIGURE 9** | AUC-ROC curve for RF-ML model.

The accuracy average of the testing set data results ranging from 0.886792 to 0.981132 for different ML-based models is shown in **Table 2**. KNN accuracy was 0.886792 for the testing set, 0.943396 for the SVM, 0.962264 for the LR, and 0.9881132 for the RF. Moreover, the area under the curve (AUC) for each of the receiver operator characteristic (ROC)

curves obtained by LR and DT was 0.976744, whereas for RF, it was 0.988095. As per the abovementioned results, when it came to the classification of OCTID, the RF performed as the best classifier.

**Figure 6** shows that RF achieved the highest percentage of accuracy out of the six ML algorithm models for correctly classifying the OCT image dataset for normal and AMD images, followed by LR, DT, SVM, NB, and KNN. The worst performance in the classification of OCT image datasets for normal and AMD is KNN. However, while RF and KNN have a significant performance difference at the 10% significance level, there is no critical efficiency difference among DT, LR, and RF.

A confusion matrix is a matrix that describes the overall performance of an ML model. The following metrics namely accuracy, precision, recall, F1 score, and ROC can be calculated from the confusion matrix. A confusion matrix for the RF model, shown in **Figure 7**, was also created to better understand which of the categories of normal retinal and AMD were confused. This was repeated for the model with and without normalization. From the graph in **Figure 7A, B** plotted for all performance metrics and output obtained without normalization, we can conclude that the RF-ML model gives better output in almost all cases.

In the case of two-class classification, RF-ML model gives a 98% precision score in normal retinal (0) images, whereas it gives a 100% precision score for AMD retinal (1) images, as shown in **Figure 8**.

For the binary classification of OCTID, the performance of the ML classifier will be related by the AUC of ROC curve. The AUC for the RF-ML model was 0.9583. Since the AUC value is close to 1 (high), the RF-ML classifier model predicts that overall performance is better in classification between AMD and normal retina of OCT images, as shown in **Figure 9**.

## Conclusion

The main contribution of this work is that suitable ML-based classifier models with their algorithms can be used to classify OCT image dataset (OCTID), consisting of AMD and normal retinal. Different ML classifier models were used to evaluate the classification metrics on OCTID. The accuracy average of the testing dataset results ranged from 0.886792 to 0.981132 for various ML-based models. KNN accuracy was 0.886792 for the testing set, 0.943396 for the SVM, 0.962264 for the LR, and 0.9881132 for the RF. The AUC for one of the ROC curves obtained by the LR and DT was 0.976744, whereas AUC for RF was 0.988095. From the abovementioned results, for the classification of OCTID, the RF performed as the best classifier in classifying AMD and normal retinal. Other metrics (precisions, recalls, and F1-scores) are also obtained by RF, LR, SVM, and KNN.

KNN is the worst performer in the classification of OCTID for normal and AMD. The results of ML-based models RF, DT, LR, SVM, and NB obtained by classification metrics with appropriate algorithm were effective and convenient in classifying OCT images of normal retinal and AMD. Finally, the RF performed the best in classifying OCT images of AMD retinal and normal retinal.

## References

1. Department of Economic and Social Affairs. *World population prospects the 2019 revision key findings and advance tables*. New York: Department of Economic and Social Affairs (2019).
2. National Eye Institute. *Facts about age-related macular degeneration*. (2021). Available online at: [https://nei.nih.gov/health/macularden/gen/armd\\_facts](https://nei.nih.gov/health/macularden/gen/armd_facts). (accessed April 21, 2022).
3. Koh J, Acharya U, Hagiwara Y, Raghavendra U, Tan J, Sree S, et al. Diagnosis of retinal health in digital fundus images using continuous wavelet transform (CWT) and entropies. *Comput Biol Med.* (2017) 84:89–97.
4. Wang Y, Zhang Y, Yao Z, Zhao R, Zhou F. Machine learning based detection of age-related macular degeneration (AMD) and diabetic macular edema (DME) from optical coherence tomography (OCT) images. *Biomed Opt Exp.* (2016) 7:4928–40.
5. Latha S, Samiappan D, Kumar R. Carotid artery ultra-sound image analysis: a review of the literature. *Proc Instit Mech Eng Part H J Eng Med.* (2020) 234:417–43. doi: 10.1177/0954411919900720
6. Kuresan H, Samiappan D, Masunda S. Fusion of mfcc feature extraction in parkinsons disease diagnosis. *Technol Health Care.* (2019) 27:363–72. doi: 10.3233/THC-181306
7. Monika R, Dhanalakshmi S, Sreejith S. Coefficient random permutation based compressed sensing for medical image compression. *Lecture Notes Electr Eng Adv Electr Commun Comput.* (2016) 2016:529–36. doi: 10.1007/978-981-10-4765-7\_56
8. Samiappan D, Chakrapani V. Classification of ultrasound carotid artery images using texture features. *Int Rev Comput Soft.* (2013) 8:933–40.
9. Rajinikanth V, Sivakumar R, Hemanth DJ. Automated classification of retinal images into AMD/non-AMD Class - a study using multi-threshold and Gaussian-filter enhanced images. *Evol. Intel.* (2021) 14:1163–71.
10. Peyman G, Roy P, Parthasarathy MK, Lakshminarayanan V. OCTID: optical coherence tomography image database. *Comput Electr Eng.* (2020) 81:2020.
11. Wong WL, Su X, Li X, Cheung CMG, Klein R, Cheng C-Y, et al. Global prevalence of age-related macular degeneration and disease burden projection for 2020 and 2040: a systematic review and meta-analysis. *Lancet Global Health.* (2014) 2:e106–16.
12. Garrfa-Floriano A, Ferreira-Santiago A, Camacho-Nieto O, Yanez-Marquez C. A machine learning approach to medical image classification: detecting age-related macular degeneration in fundus images. *Comput Electr Eng.* (2019) 75:218–29.